Research Article

He Wang and Liguo Chen*

Novel electrodes for precise and accurate droplet dispensing and splitting in digital microfluidics

https://doi.org/10.1515/ntrev-2021-0054
received May 5, 2021; accepted July 21, 2021

Abstract: Digital microfluidics (DMF) is a versatile fluid handling tool that is widely used in the biochemical field. There are very high requirements for the volume of single droplet in many biochemical applications. Droplet dispensing and splitting are two main operations to generate a single droplet in DMF. Therefore, the generation of droplets with high volume precision and accuracy in the two droplet operations is one of the keys to the efficient application of DMF in biochemical analysis. We have developed a novel droplet dispensing and splitting scheme where electrode geometry is optimized. The liquid column can contract in a regular shape, which keep the neck shape uniform and stable, and the position of pinch-off point was fixed; meanwhile, the liquid tail is eliminated before pinching off, so that the precision and accuracy of droplet volume were greatly improved. The increase in the radius of the cutting electrodes elongated the droplet neck and increased the neck curvature at the pinch-off point, which further effectively improved the precision and accuracy of droplet volume. The optimized droplet splitting scheme can also be applied to the droplet splitting with unequal volume effectively.

Keywords: digital microfluidics, electrode geometry optimization, dispensing, splitting, volume precision, volume accuracy

1 Introduction

Digital microfluidics (DMF) for microdroplet control has been widely used in the fields of biology, medicine, analytical chemistry, food safety, and environment [1–3]. DMF has the capacity to address each droplet individually with no need for complex networks of channels, pumps, microvalves, or mechanical mixers [4]. The droplets containing cells, proteins, DNA, or other reagents can be manipulated on a centimeter level planer chip for various analysis and detection in routine biomedical laboratories, which is termed as on-chip experiment. In all applications, on-chip experiments usually consist of a series of droplet operations, including droplet dispensing, transporting, mixing, splitting, and online or offline detections. DMF has the capacity to address each droplet individually [4]. It can effectively avoid the cross-contaminations, greatly reduce reagent and/or sample consumption and the time of biochemical reactions, and achieve precise quantitative control. In DMF devices, discrete droplets are typically manipulated by applying a series of electrical potentials to an array of electrodes coated with a dielectric layer and a hydrophobic layer, which is referred to as EWOD, one of the most commonly actuation mechanisms.

DMF chips have two different configurations (Figure 1): the closed configuration [5] and the open configuration [6]. Due to dynamic reconfigurability, different droplet operations can be implemented in different time span on the same set of electrode cells. Also, the same droplet operation can also be relocated onto other position in the array in another time span with dynamic reconfigurability [7,8].

All operations in DMF are performed for single or multiple working droplets. The volume of a working droplet is very important because it has great influence on many parameters such as flow rate, concentration, and energy conversion of itself. Therefore, there is a pressing need to improve volume precise and accuracy of a single droplet in the on-chip experiments. Volume precision (*i.e.*, reproducibility) of the droplet refers to the volume consistency of droplets that are repeatedly generated

* **Corresponding author: Liguo Chen,** Robotics and Microsystem Center, School of Mechanical and Electrical Engineering, Soochow University, Suzhou 215006, China, e-mail: chenliguo@suda.edu.cn
He Wang: Robotics and Microsystem Center, School of Mechanical and Electrical Engineering, Soochow University, Suzhou 215006, China; School of Mechanical Engineering, Henan University of Engineering, Zhengzhou 451191, China

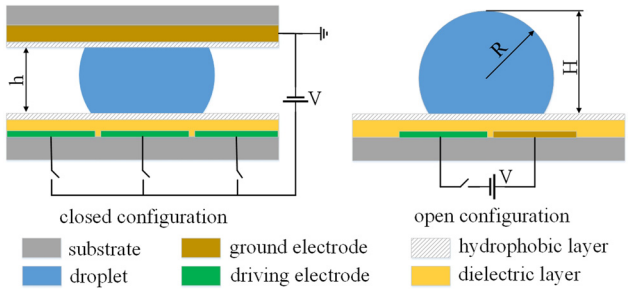

Figure 1: Side-view schematics of closed (left) and open (right) configuration.

under the same conditions, which is defined by the mean and the standard deviation of a group of droplet volumes (usually no less than ten measurements). The higher the volume precision, the lower the volume inconsistency. Herein, volume inconsistency is used to evaluate volume precision. Relative standard deviation (RSD) (standard deviation divided by the mean) is commonly used to indicate the volume inconsistency in practical analysis. In some applications such as drug discovery, the required RSD should be less than 10%, preferably less than 5%, while the requirement is more stringent for microdialysis applications, with an RSD of below 2% [9,10]. Volume accuracy of the droplet refers to the closeness between the actual generated volume of a single droplet and its target volume. The higher the volume accuracy, the lower the inaccuracy. Herein, the inaccuracy is defined by the relative error (RE) between the volume mean of droplets that are repeatedly generated and the target volume and calculated as follows:

$$\mathrm{RE} = (\mathrm{VM} - \mathrm{TV})/\mathrm{TV}, \tag{1}$$

where VM is the volume mean of droplets and TV is the target volume. For most applications, it is appropriate to control the volume inaccuracy within 5% [9].

There are two ways to generate a single droplet in DMF: droplet dispensing and droplet splitting. In the basic droplet operations of DMF, dispensing and splitting are more difficult to implement than transporting and mixing, because they require specific criteria in terms of electrode geometry and electrical aspects [7]. Droplet dispensing is often the first step in the on-chip experiments. The volume of the initial droplet is controlled by the dispensing operation, which greatly affects the accuracy of subsequent droplet operations. As far as I know, three droplet dispensing schemes have been reported so far. The first one is to dispense working droplets directly from the reservoir [2,11,12], the second one uses an additional syringe pump with precise volume control for droplet dispensing [13,14], and the third one is to perform dispensing operation through capacitance feedback [10,15–17]. In the direct dispensing scheme, the droplet volume is affected by many factors among which the geometry of the electrodes used for the droplet dispensing and their location settings are two main factors. In DMF chips, square electrodes are usually used for dispensing operation. Although it is relatively simple to implement, it is difficult for square electrodes to dispense droplets with high volume precision and accuracy. Cho *et al.* introduced two side electrodes on both sides of the main fluid path to fix the position of pinch-off point, thereby improving the volume consistency of the dispensed droplets [7]. Yaddessalage designed a TCC reservoir [18] and Nikapitiya *et al.* proposed a L-junction reservoir [19] to obtain the droplet with high volume precision and accuracy, but the same problem exists in the two electrode optimization schemes, that is, the control of the electrodes is too complicated in the droplet dispensing process. The use of the external syringe pump can effectively reduce the volume error of the dispensed droplet below 1%, but it not only increases the control complexity, but also is not conductive to efficient integration, which limits its application. The dispensing scheme with capacitance feedback can effectively reduce droplet volume error, but the introduction of capacitance feedback increases the complexity of DMF system. Therefore, we still focus on the direct droplet dispensing scheme in this work.

Droplet splitting plays an important role in dilution and concentration of droplets and separation of particles from droplet, which facilitates the application of DMF chip in the field of biochemical analysis. In the traditional three-square-electrode splitting scheme, the volumes of the two child droplets are unequal and the error is large due to the initial position of the mother drop deviating from the center of the middle electrode and its uneven shrinkage. Nikapitiya *et al.* proposed a Y-junction splitting unit so that it preformed symmetric and faster droplet splitting and the volume inconsistency of two child droplets is much less than 1% [19]. However, the optimized scheme has two disadvantages: one is that the control of the electrodes is complex and the other is that the droplet splitting operation can only be carried out in a single direction. Dong *et al.* designed a 3D microblade structure for precise and parallel droplet splitting [20], but the chip fabrication process was complex and the driving voltage was too high. Table 1 summarizes the above-mentioned studies that have been reported to improve the volume precision and accuracy of the dispensed or split droplets.

Therefore, based on the principle of not increasing the difficulty of fabrication process and integration of the

Table 1: Reported different method to improve volume precision and accuracy of a single droplet

Operation	Method	Results	Reference	Comments
Dispensing	Capacitance metering	Volume error: 1.2%	Ren and Fair, 2002 [15]	Both volume precision and accuracy data
Dispensing	Real-time feedback control	Volume error: <±1%	Gong and Kim, 2006 [16]	Both volume precision and accuracy data
Dispensing	Chips were fabricated *via* electrical wiring on the multilayer PCB to eliminate side connection lines, and simple electrical signal switching or changing the drive voltage was used to adjust the droplet volume	The lowest volume error: ±5%	Gong and Kim, 2006 [17]	Only volume accuracy, but no precision data
Dispensing	Analysis of the response of multiple factors, such as cutting electrode and applied voltage to droplet volume and reproducibility	Volume variation: 3.0%	Wang *et al.*, 2010 [21]	Only volume accuracy, but no precision data
Dispensing	Optimization of the dispensing electrode shape and layout: (a) TCC reservoir design; (b) enhance TCC reservoir design	(a) Volume error: 3.7% (b) Volume error: 0.085%	Yaddessalage, 2013 [18]	Both volume precision and accuracy data
Dispensing	Optimization of the dispensing electrode shape and layout: L-junction reservoir design	Inaccuracy: 0.17% Inconsistency: 0.10%	Nikapitiya *et al.*, 2017 [19]	Both volume precision and accuracy data
Splitting	Optimization of the splitting electrode shape and layout: C-junction splitting design and Y-junction splitting design	Volume error: 0.98%	Yaddessalage, 2013 [18]	Only volume accuracy, but no precision data
Splitting	Optimization of the splitting electrode shape and layout: Y-junction splitting design	Inaccuracy: 0.85% Inconsistency: 0.025%	Nikapitiya *et al.*, 2017 [19]	Both volume precision and accuracy data
Splitting	The use of a 3D microblade structure	Volume variance from 1.7% (150 V_{rms}) to 0.4% (300 V_{rms})	Dong *et al.*, 2017 [20]	Only volume accuracy, but no precision data

DMF chip, we optimized the geometry of the electrodes used for droplet dispensing and splitting to improve the volume precision and accuracy of a single droplet and compared the droplet volume before and after optimization.

2 Basic principles of electrode optimization

Droplet dispensing process is very similar to droplet splitting, but the former is much more challenging. In traditional direct dispensing scheme, a square reservoir stores a large amount of liquid, and small droplets can be dispensed from it by electrowetting-on-dielectric (EWOD), as shown in Figure 2a. First, the electrodes have to be activated sequentially from left to right to pull out a liquid column from the reservoir and onto the target dispensing electrode; and then, the target dispensing electrode and the reservoir electrode are activated while the electrodes between them are deactivated; finally, a droplet is dispensed just at the target dispensing electrode. Figure 2a(3–5) show three different dispensing positions. It is found that the dispensing process was unstable. Ideally, the liquid should contract symmetrically in the arc-shape manner and pinch off at the equilibrium. However, the liquid column cannot contract and cut off as desired in the actual dispensing operation due to the imperfect surface of the DMF chip and the rapid pinch off at the neck. Moreover, even if the size of the dispensing electrode at different location is the same, the length of the liquid tail is inconsistent and the volume is changed due to the inconsistent length of the liquid column drawn from the reservoir and the unfixed position of the pinch-off point. After the droplet is pinched off, the liquid tail with variable volume is added to the dispensed droplet, which results in the actual volume of repeated dispensed droplets to be inconsistent and larger than that of the target electrode. In the dispensing operation, the volume corresponding to the target electrode is the target volume, which is equal to the product of the area of the target electrode and the spacing between the top and bottom plates. Therefore, the most direct way to improve the volume precision and accuracy of the dispensed droplets is to increase the stability of the droplet generation process. To achieve this goal, a set of electrodes used for dispensing should meet the following three criteria:

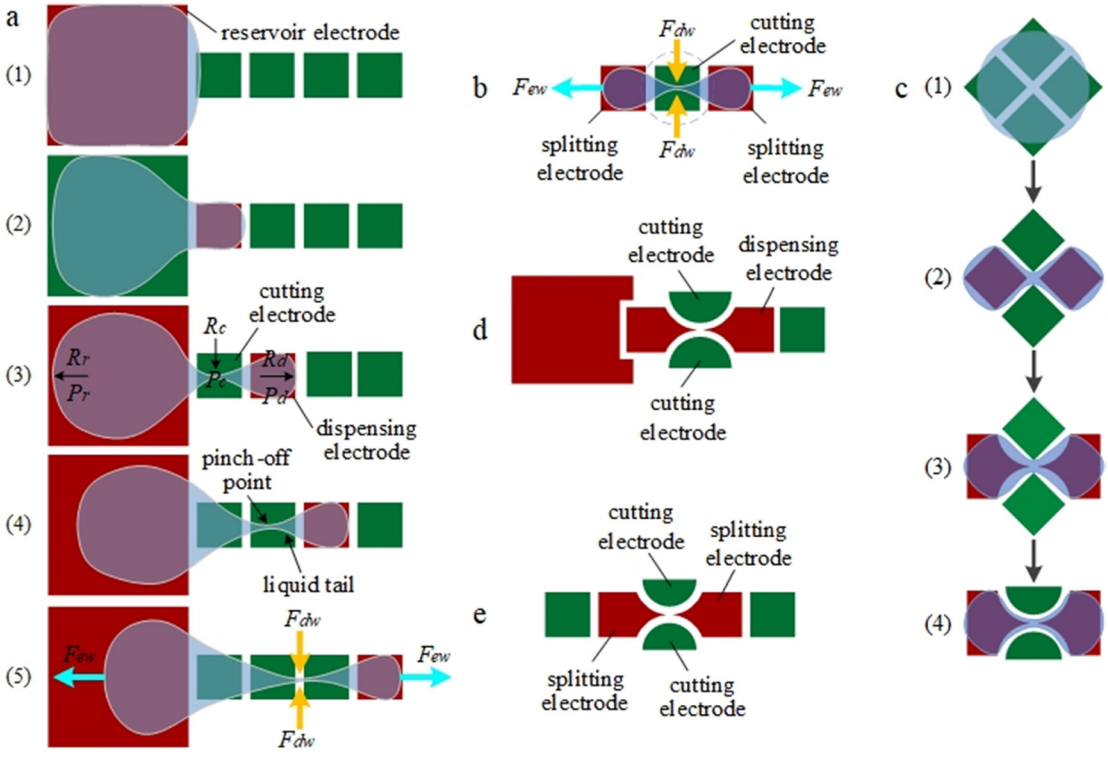

Figure 2: Droplet dispensing and splitting scheme. (a and b) Traditional dispensing and splitting scheme with square electrodes. (c) Ideal droplet separation concept and its evolution. (d) Optimized droplet dispensing scheme. (e) Optimized splitting schemes. The activated electrode is shown in red, while the deactivated electrode is shown in green.

(1) the liquid column can contract in a regular shape;
(2) shorten the length of the liquid tail as much as possible, and if possible, eliminate the liquid tail completely, which requires the contraction shape to be the same as that of the dispensing electrode;
(3) the liquid column can be pinched off at a fixed position.

Droplet splitting also has some problems similar to droplet dispensing. When the initial center of the mother droplet deviates from the center of the cutting electrode, its coverage area on the activated electrode at both ends is unequal, so the electrowetting forces acting on both sides of the mother droplet are not uniform, resulting in splitting into two child droplets with unequal volume. If the initial center of the mother droplet deviates too much from the center of the cutting electrode, the mother droplet is even pulled to one side, so that the splitting operation cannot be implemented. Further, the huge EWOD force leads to the rapid splitting of the mother droplet, so that the middle area of the droplet may not become a thin neck and a small residue may be left on the middle electrode after splitting [22,23]. Therefore, whether it is the dispensing operation and the splitting operation, there is a pressing need to optimize the traditional dispensing and splitting scheme with square electrodes to improve the volume precision and accuracy of the generated droplets.

In the process of droplet dispensing and splitting, since the left and right electrodes covered by the initial droplet are activated and the middle electrode is deactivated, the two ends of the droplet are hydrophilic while the middle part is hydrophobic, which inevitably causes the droplet to be elongated along the longitudinal direction and the meniscus on the middle electrode begins to contract so as to keep the volume of the initial droplet constant. Therefore, the droplet dispensing and splitting operations are caused by droplet elongation in the longitudinal direction and the necking (the neck curvature R_c is negative [7]) in the middle. According to the Laplace pressure equation, there are $P_r - P_a > 0$ and $P_d - P_a > 0$ at both ends of the droplet, and $P_c - P_a < 0$ at the neck. As a result, the droplet is subjected to a pair of dewetting forces (F_{dw}) that exert a squeezing effect at the neck, while it is subjected to a pair of electrowetting forces (F_{ew}) playing a pulling effect at the two sides, as shown in Figure 2a(5) and 2b. Therefore, the increases in the neck length and the neck curvature favor dispensing and splitting. Beside, the small spacing between the top and bottom plate is also conducive to droplet separation [7,21]. However, the elongation of neck will inevitably increase the length of the liquid tail in traditional scheme, which will decrease the precision and accuracy of the generated droplet. Therefore, how to optimize the electrode geometry to increase the neck curvature and elongate the neck without increasing the tail length is critical to achieve high-performance droplet dispensing and splitting operation. We believe that pinching off the droplet along the diagonal of square electrode is more suitable for the two droplet operations, as shown in Figure 2c(1 and 2), which is consistent with the ideal droplet separation concept in the literature [19]. Such a droplet separation strategy can fix the position of the pinch-off point, which satisfies the third criterion. On this basis, the electrode shape was further optimized. As can be seen from Figure 2a and b, the contour shape of the droplet at the neck is like an arc. To ensure that the droplet can always contract in a regular shape, the shape of the electrode is optimized as a circular arc, which also nearly eliminates the liquid tail after the droplet pinching off, as shown in Figure 2c(3 and 4), which makes the droplet separation satisfy the first two criteria. Therefore, a droplet dispensing scheme (Figure 2d) and a droplet splitting scheme (Figure 2e) were designed. In the following, the optimized droplet dispensing and splitting schemes are verified by experiments and compared with the traditional dispensing and splitting schemes with square electrodes in terms of the precision and accuracy of the generated droplets.

3 Methods

3.1 DMF chip fabrication and system integration

The chip was fabricated by our recently developed rapid prototyping technology [24] for DMF. The array of patterned electrodes was designed by vector drawing software, and then converted into 1-bit TIF diagram that was input into a microelectronic circuit printer (BroadJET L3000, Beijing BroadTeko Intelligent Technology Co., Ltd). The electrode layer was formed by inkjet printing nanosilver particle conductive ink on PET sheet. In order to improve the conductivity, multilayer printing mode was adopted, and then the printed substrate was sintered at 120°C for 30 min in an electric thermostatic drying oven after the last printing. The PMP cling wrap was used as the dielectric layer. The cling wrap was cut to the required size, and then Teflon® AF 1600 was curtain-coated on it

with a disposable plastic dropper. The printed PET substrate was fixed onto the glass slide to ensure the flatness of the flexible DMF chip, and then the cling wrap coated with Teflon® AF was tightened and adhered onto the glass slide with double-side tape until there is no wrinkle to form the dielectric and hydrophobic layer. To guarantee that the cling wrap can be tightly attached to the electrode surface without air bubbles, a thin layer of silicone oil was spread onto the electrode array and the substrate before cling wrap was taped on the glass slide. As the top plate, ITO-coated glass slide was immersed in Teflon® AF so that a layer of Teflon can be deposited on the surfaces of the top plate. Double-side tape is used as a spacer to control the spacing between the top and bottom plates.

Since the droplets are in between parallel plates with a small spacing during all the experiments, generated droplets can be approximately regarded as a cylinder. The volume of generated droplets can be calculated by the product of the spacing between the top and bottom plates and the contact area of the droplet on the top plate (*i.e.*, the footprint area). The top view of the droplets was captured by an industrial camera (the frequency of image capture is 60fps), and then the images were imported into the image processing software (Image J) for calculating the footprint area. In addition, a 32-bit relay control board was used as a switching device to realize on-off control of each electrode to implement all droplet operations.

3.2 Test and control methods

The precision and accuracy of droplet volume in traditional dispensing and splitting schemes with square electrodes, an optimized dispensing scheme, and an optimized splitting scheme have been investigated. In all the experiments, ten droplets were dispensed or split in turn, and the volume of the generated droplets was calculated. The area of traditional square reservoir electrode is $2.5\,mm^2 \times 2.5\,mm^2$, and that of all small square electrodes is $1\,mm^2 \times 1\,mm^2$. For the optimized dispensing scheme, the area of reservoir electrode is about $6.24\,mm^2$. The liquid in all experiments is potassium permanganate solution.

For the dispensing operation, the electrode control method in the traditional scheme and the optimized scheme is shown in Figures 2a and 3a, respectively. In the latter, the electrodes R, A_1, S_1/S_2, and A_2 were activated in sequence, and the liquid column was pulled out from the reservoir by electrowetting force until these electrodes were filled with the liquid; and then the electrodes R, A_1, and A_2 were activated while the cutting electrodes S_1 and S_2 were deactivated, and two dewetting menisci moved toward each other to form a neck until the neck contracted to be pinched off, generating a droplet at the dispensing electrode A_2.

In practical biochemical analysis, two or more droplets are often mixed and then split according to actual demand. All the splitting experiments were carried out according to the principle that the droplets were mixed first and then split, so it could not be guaranteed that the mother droplet to be split was completely located at the center of the cutting electrode, and its initial position was not deliberately adjusted during the experiment. For the splitting operation, two electrode control modes were used in the traditional scheme. Mode I was to directly activate the splitting electrodes on both sides of the mother droplet, while the middle cutting electrode was deactivated; mode II is to activate the three electrodes at the same time, and then deactivate the middle electrode after the mother liquid droplet was elongated (Figure 3b). In the optimized splitting scheme, after mixing the initial

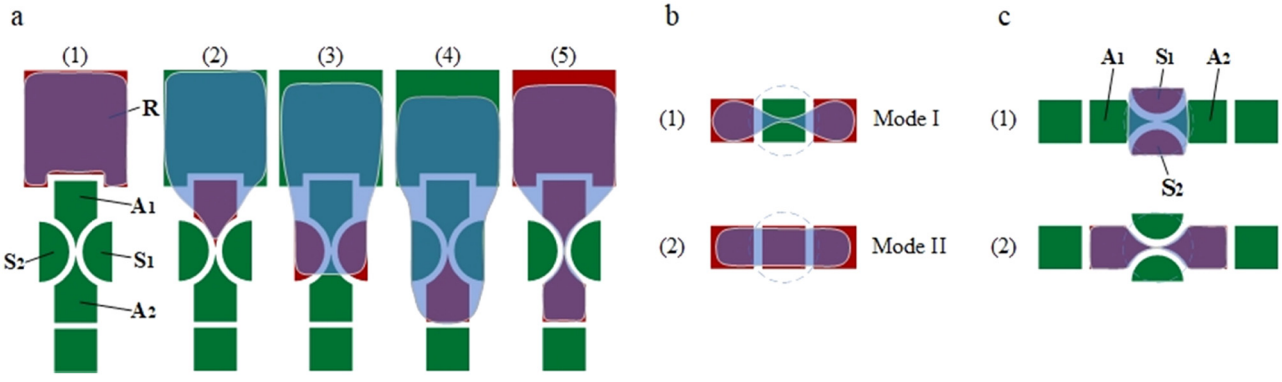

Figure 3: Electrode control mode in droplet dispensing and splitting schemes: (a) Optimized droplet dispensing scheme; (b) traditional droplet splitting scheme with square electrodes; (c) optimized droplet splitting scheme.

two droplets into a mother droplet by activating cutting electrodes S_1 and S_2, activated splitting electrodes A_1 and A_2 while deactivated S_1 and S_2 to split it, generating two child droplets, as shown in Figure 3c.

4 Results and discussion

4.1 Droplet dispensing

Figure 4(a–f) demonstrates the droplet dispensing process using the optimized electrode scheme in which the radius of the semicircular cutting electrodes is 0.7 mm. The sequential activation of the electrodes created a continuous electrowetting force that pulled a liquid column out of the reservoir. Once the dispensing electrode was filled with the liquid, two cutting electrodes were deactivated, so that two dewetting menisci contract inward and the neck width gradually decreased. We can observe from Figure 4e that the shape of the two dewetting meniscus after complete contraction was consistent with that of the cutting electrode, which allows the neck contraction shape to remain stable and uniform, forcing the liquid column to be pinched off at a fixed point. As a result, a droplet with high volume precision and accuracy was generated at the dispensing electrode(Figure 4f). Figure 4g–j show the process of dispensing the fifth and tenth droplet. To further analyze the performance of the optimized dispensing scheme, the cutting electrodes with the radius of 1.2, 1.6, and 2.0 mm were used to dispense droplets from the reservoir, as shown in Figures 5–7.

Figure 8 summarizes the volume analysis results of droplet dispensed from the reservoir using the optimized scheme and the traditional scheme. The volume error of the droplets dispensed by the square electrodes is nearly 9%, and the average volume is about 27% more than the target volume, and the maximum error is as high as about 41%. After the optimization of the electrodes, the volume precision and accuracy are greatly improved. For the cutting electrode radius of 0.7, 1.2, 1.6, and 2.0 mm, the inaccuracy of droplet volume is about 2.74, 2.14, 1.58, and 1.33%, respectively, while the inconsistency is about 1.60, 1.05, 0.819, and 0.532%, respectively. The neck length increases with the increase in the radius of the cutting electrode, and the volume of the droplets actually dispensed fluctuates less, so the volume precision and accuracy are improved. Furthermore, the increase in the radius of the cutting electrode causes the liquid column to be stretched longer during the pinch-off process, and the shape of the neck becomes more and more consistent with that of the cutting electrode, so that the neck becomes thinner and the droplets are more likely to be pinched off. One-way analysis of variance (one-way ANOVA) was used to analyze whether the cutting electrode radius has a significant influence on the droplet volume. The significance level (α) of the difference between the average values was set to 0.05 and multiple comparison analysis was performed. From the F-test critical value table, the F critical value with degrees of freedom (3,36) can be obtained as $F_{0.05}(3,36) = 2.866$. As shown in Figure 8, $F \gg F_{0.05}(3,36)$, and the significance value p between any two radius groups is less than α, which indicates that there are significant differences between the four cutting electrode radius groups. Therefore, the radius of the cutting electrode has a significant influence on the droplet volume.

For the four selected radii of the cutting electrode, even for the smallest radius (0.7 mm), the precision and accuracy of the dispensing droplet volume are much higher than those of the traditional square electrodes, which indicates that the optimized dispensing scheme has distinct advantages and the increase in the neck length is more conducive to droplet dispensing. The

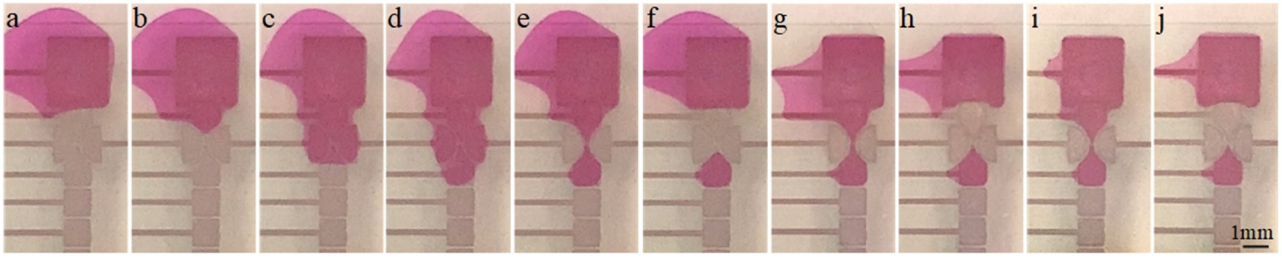

Figure 4: Series of video frames displaying the process of dispensing a droplet from a reservoir using the optimized electrodes scheme with the cutting electrodes radius R = 0.7 mm; (a–d) A liquid column was drawn from the reservoir as the electrodes are activated in turn; (e) Cutting electrodes were deactivated to form a neck; (f) The first droplet was generated at the dispensing electrode; (g and h) The fifth droplet was dispensed; (i and j) The tenth droplet was dispensed.

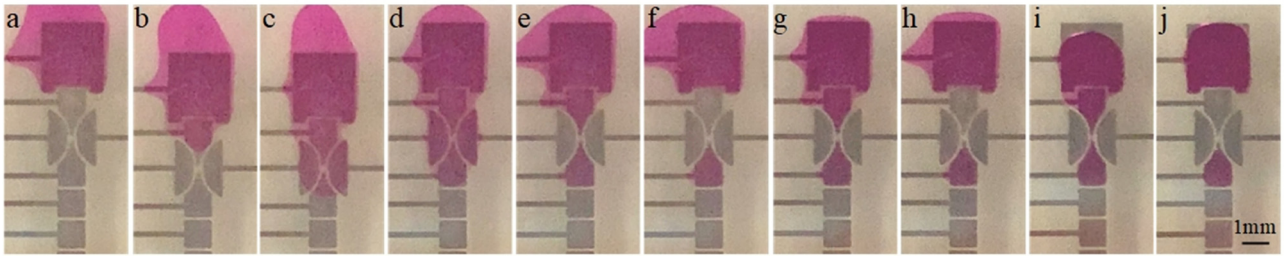

Figure 5: Series of video frames about droplet dispensing using the optimized electrodes scheme with the cutting electrodes radius R = 1.2 mm (Video S1); (a–f) The first droplet was generated; (g and h) The fifth droplet was dispensed; (i and j) The tenth droplet was dispensed.

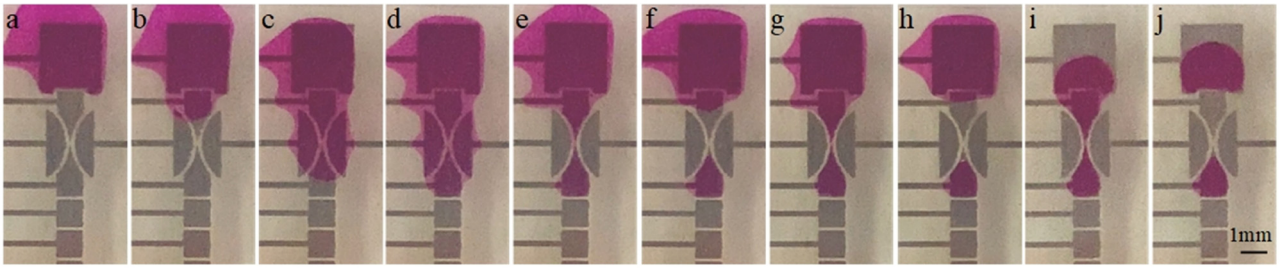

Figure 6: Series of video frames about droplet dispensing using the optimized electrodes scheme with the cutting electrodes radius R = 1.6 mm; (a–f) The first droplet was generated; (g and h) The fifth droplet was dispensed; (i and j) The tenth droplet was dispensed.

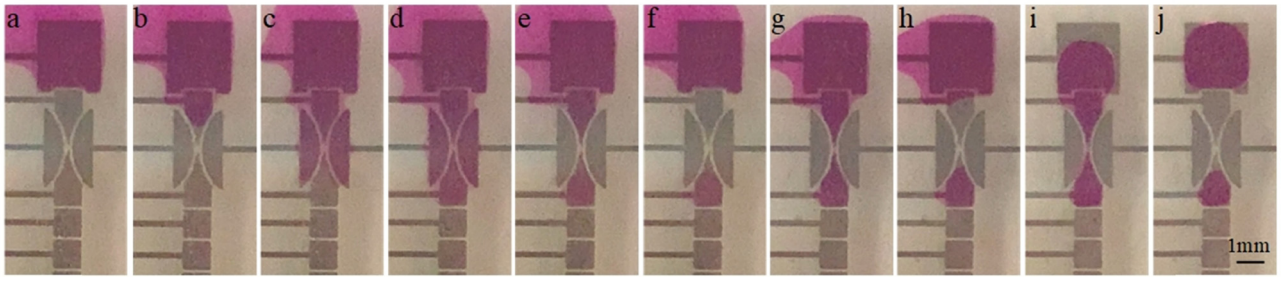

Figure 7: Series of video frames about droplet dispensing using the optimized electrodes scheme with the cutting electrodes radius R = 2.0 mm (Video S2); (a–f) The first droplet was generated; (g and h) The fifth droplet was dispensed; (i and j) The tenth droplet was dispensed.

significant improvement in droplet dispensing performance in the optimized scheme is mainly attributed to the stability of the dispensing process, that is, the fixed position of the pinch-off point, the elimination of the liquid tail, and the consistent contraction shape of the neck.

4.2 Droplet splitting

The performances of the traditional splitting scheme with square electrodes and the optimized droplet splitting scheme were compared through experiments. For the traditional splitting scheme, it was found that the droplet was often pulled to one side in the electrode control mode I. This is mainly because the coverage area of the mother droplet on the two adjacent electrodes is unequal in the initial state. Once the splitting electrodes on both sides are activated, the electrowetting force acting on the mother droplet is not balanced, causing it to flow toward the side with a larger coverage area. The electrode control mode II is slightly better than the mode I. This is because the three electrodes can be activated simultaneously to elongate the droplet, and the coverage area of the elongated droplet on the adjacent electrodes on both sides increases; after the middle cutting electrode is deactivated, the part of the mother droplet that is not controlled

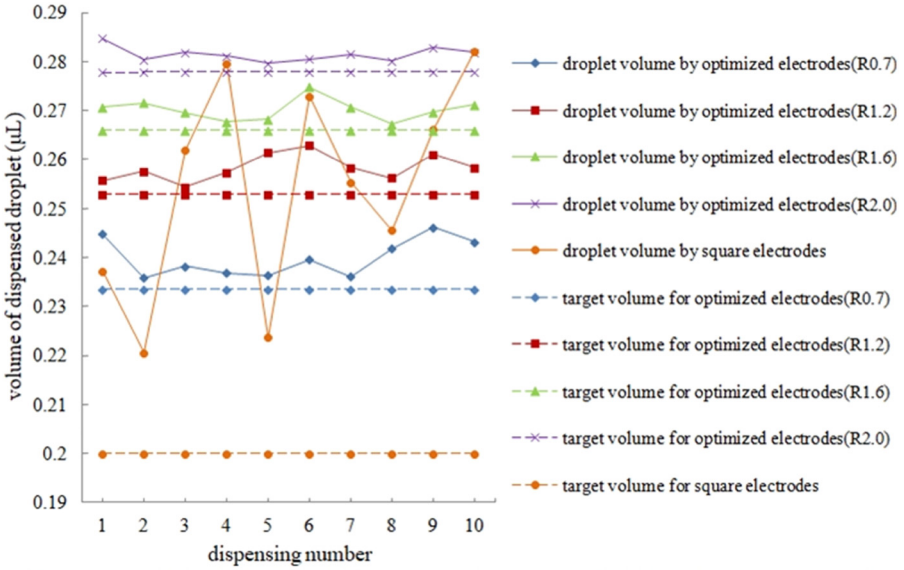

Comparison of inconsistency and inaccuracy in droplet volume					
	optimized dispensing scheme				Traditional scheme
	R=0.7mm	R=1.2mm	R=1.6mm	R=2.0mm	
mean	0.240	0.258	0.270	0.282	0.255
STD	0.00384	0.00272	0.00221	0.00150	0.0221
inaccuracy(%)	2.74	2.14	1.58	1.33	27.3
inconsistency(%)	1.60	1.05	0.819	0.532	8.67

ANOVA test of droplet volume	
F	432.170
Significance (p)	<0.001

Figure 8: The volume of the dispensed droplets for optimized electrodes and traditional square electrodes.

by the electrodes decreases, so that the droplet state is relatively more stable. In both cases, the shape of the neck formed in the middle of the mother droplet is unstable after the middle electrode is deactivated, and the position of the pinch-off point is not fixed. Therefore, the two child droplets are not equal in volume and there is also a large volume inconsistency.

Figure 9 depicts the process of splitting a mother droplet into two child droplets with the optimized electrodes scheme in which the radius of the cutting electrodes is 0.7, 1.2, 1.6, and 2.0 mm, respectively. Figure 10 compares and analyzes the experimental results of the traditional and optimized splitting scheme. It can be seen that the volume inconsistency of the child droplets in the two modes of the traditional splitting scheme is very high, but the mode II is slightly better than the mode I. Compared with the traditional scheme, the optimized splitting scheme can provide better splitting performances in

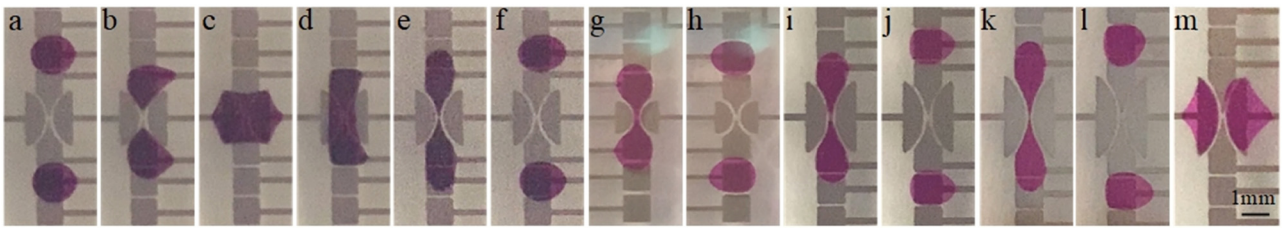

Figure 9: Series of video frames displaying the process of splitting a mother droplet into two child droplets using the optimized electrodes scheme; (a–f) The cutting electrodes radius R = 1.2 mm; (g and h) The cutting electrodes radius R = 0.7 mm; (i and j) The cutting electrodes radius R = 1.6 mm (Video S3); (k–m) The cutting electrodes radius R = 2.0 mm (Video S4).

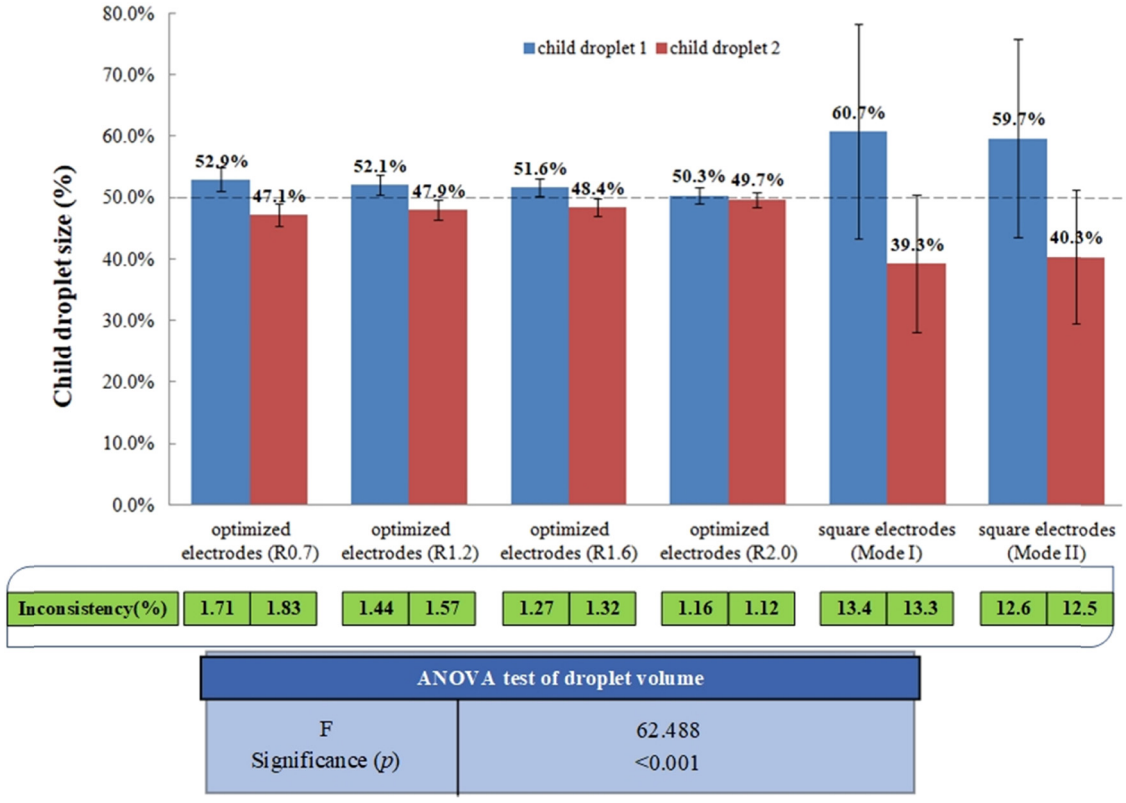

Figure 10: The volume of the child droplets for optimized splitting electrodes and traditional square splitting electrodes. The child droplet 1 refers to the larger one, while the child droplet 2 refers to the smaller one.

terms of volume precision of a single child droplet and the volume consistency of two child droplets. The volume inconsistency of the single child droplet decreases seven times from 13.3 to 1.8%. Moreover, the volume precision of the child droplet improves with the increase in the neck length, which is similar to that of droplet dispensing. Figures 9 and 10 clearly confirm that the success of the optimized splitting scheme to split droplets with high volume precision lies in the fact that it not only manages to significantly eliminate the liquid tail, but also that the contraction shape of the mother droplet closely resembles that of the cutting electrodes, and more importantly, that it can also fix the position of the pinch-off point. As a result, the volume of the two child droplets is almost equal. The one-way ANOVA is also used to analyze whether the cutting electrode radius has a significant effect on the volume of the split droplet. The significance level α is also set to 0.05. As shown in Figure 10, $F > F_{0.05}(3,36)$ and $p < \alpha$, which indicate that there are significant differences between the four cutting electrode radius groups in the optimized droplet splitting scheme. Therefore, the radius of the cutting electrode has a significant effect on the volume of the split droplet.

It was found in the splitting experiments that as the radius of the cutting electrode increases, two droplets might move onto the two cutting electrodes separately and the mixing operation cannot be completed if the volume of the droplet before mixing was a little small (Figure 9m). Therefore, the appropriate cutting electrode radius should be selected according to the actual demand for the volume of the child droplets after splitting in practical applications. Even for the cutting electrode with a radius of 0.7 mm, the volume inconsistency of the child droplets is lower than the requirement for rigorous biochemical applications (<2%).

The optimized splitting electrodes not only have excellent applications in the droplet splitting with equal volume, but also can be used for the droplet splitting with unequal volume. In Figure 11a, the volume ratio between target 1 and target 2 of two child droplets in the unequal volume splitting scheme with the cutting electrode radius R = 0.7 mm was 57.3:42.7, while it was 56.8:43.2 in the scheme with the cutting electrode radius R = 1.2 mm. Figure 11b–h show the unequal volume splitting process by using two types of different cutting electrode radii (Video S5). Similar to the droplet splitting with equal

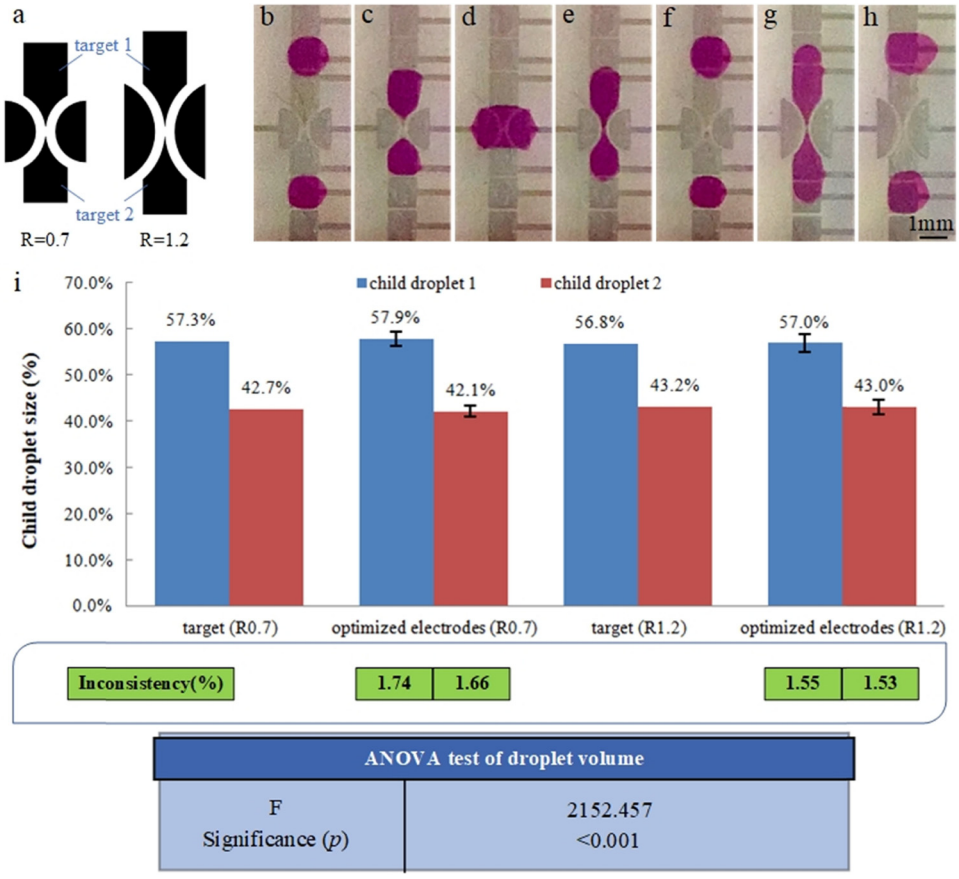

Figure 11: Droplet splitting with unequal volume using the optimized electrodes scheme; (a) Two types of optimized electrodes in which the cutting electrode radius was 0.7 and 1.2 mm, respectively; (b–f) Series of video frames displaying unequal splitting using the cutting electrode with a radius of 0.7 mm; (g and h) Series of video frames displaying unequal splitting using a cutting electrode with a radius of 1.2 mm; (i) The volume of the child droplets for two optimized splitting electrodes. The child droplet 1 and 2 correspond to the droplet split on target electrode 1 and 2, respectively.

volume, the increase in neck length effectively decreases the volume inconsistency of the two unequal child droplets (both less than 2%), and the actual volume ratio of the two child droplets becomes closer to the target volume ratio (Figure 11i). According to one-way ANOVA, $F > > F_{0.05}(1,18) = 4.414$ and $p < \alpha = 0.05$, where $F_{0.05}(1,18)$ denotes the critical value of F with the significance level $\alpha = 0.05$ and the degree of freedom (1,18). Therefore, the cutting electrode radius also has a significant effect on the volume of the child droplet with unequal splitting.

4.3 Comparison with the reported scheme

As mentioned earlier, some studies have proven that a variety of methods can be used to improve the volume precision and accuracy of a single working droplet, such as optimizing the chip structure or shape and layout of dispensing and splitting electrode, and introducing capacitive feedback systems, *etc.*, as shown in Table 1. Except for the method proposed in the literature [19], the optimization scheme of the dispensing and splitting electrodes proposed in this paper is equivalent to the literatures [15,16,18,20] in terms of optimization performance, *i.e.*, volume precision and accuracy, but is superior to the methods in the literatures [17,21]. All the chips used in the experiment in Table 1 are processed by microprocessing techniques such as photolithography, so the width of electrode wires on these chips is often less than 100 µm. However, the electrode layer on the chip used in this paper is fabricated by inkjet printing. Due to the characteristics of inkjet printing technology, although the width of the electrode wires is designed to 150 µm, the actual value is greater than 150 µm [24]. In the experiments, it was found that the larger width of the electrode wire leads to the electrode wire corresponding to the dispensing and splitting electrode to trap a portion of the liquid during the process of dispensing and splitting. Therefore,

it is the electrode wire with larger width that reduces the volume precision and accuracy of the dispensed and split droplets. Although decreasing the wire width can improve the volume precision and accuracy of the droplets, it will reduce the conductivity of the electrode wires and increase the driving voltage for the droplet operations [24]. Therefore, the width of the electrode line in the paper was set as 150 μm in order not to increase the droplet operating voltage. It is because of the wider electrode wire that the volume precision and accuracy of the droplet by the electrode optimization scheme proposed in this paper is less than that of the literature [19]. We infer that if the proposed optimized electrodes are fabricated by traditional micromachining techniques to be used for droplet dispensing and splitting, the volume precision and accuracy of the droplets may not be much different from the method in the literature [19] and are better than all other methods. In addition, the electrode control is simpler than that of Table 1, especially compared with the literature [18] and [19]. The most critical point is that there is no need to increase the difficulty of chip fabrication and integrate a complex capacitive feedback system.

5 Conclusion

A novel droplet dispensing and splitting scheme is proposed. The dispensing and splitting electrodes were optimized to meet the three criteria for dispensing and splitting droplets with high volume precision and accuracy, which accords with the volume requirements of droplet dispensed and split in many biological applications. Compared with the traditional dispensing scheme with square electrodes, the volume inconsistency of droplets is decreased by at least 5 times and the inaccuracy by at least 10 times in our proposed dispensing scheme. In droplet splitting operation, the volume inconsistency of the child droplets is reduced by about 7 times by the optimized electrode scheme. The improvement of droplet dispensing and splitting performance is mainly due to the fixed position of the pinch-off point, the elimination of the liquid tail, and the uniform and stable shape of the droplet neck before pinching off. More importantly, the neck length of the droplet and the neck curvature at the pinch-off point are increased with the increase in the cutting electrode radius, which effectively improves the precision and accuracy of the droplet volume. The optimized splitting scheme can not only greatly improve the performance of equal volume splitting, but also be effectively used for the droplet splitting with unequal volume.

Funding information: The authors gratefully acknowledge the financial support of the Natural Science Foundation of the Jiangsu Higher Education Institutions of China (No. 17KJA460008).

Author contributions: All authors have accepted responsibility for the entire content of this manuscript and approved its submission.

Conflict of interest: The authors state no conflict of interest.

Reference

[1] Choi K, Ng AHC, Fobel R, Wheeler AR. Digital microfluidics. Annu Rev Anal Chem. 2012;5:413–40.
[2] Jebrail MJ, Bartsch MS, Patel KD. Digital microfluidics: a versatile tool for applications in chemistry, biology and medicine. Lab Chip. 2012;12(14):2452–63.
[3] Sista R, Hua Z, Thwar P, Sudarsan A, Srinivasan V, Eckhardt A, et al. Development of a digital microfluidic platform for point of care testing. Lab Chip. 2008;8(12):2091–104.
[4] Mugele F, Baret JC. Electrowetting: from basics to applications. J Phys Condens Mat. 2005;17(28):R705–74.
[5] Pollack MG, Shenderov AD, Fair RB. Electrowetting-based actuation of droplets for integrated microfluidics. Lab Chip. 2002;2(2):96–101.
[6] Washizu M. Electrostatic actuation of liquid droplets for microreactor applications. IEEE Trans Ind Appl. 1998;34(4):732–7.
[7] Cho SK, Moon H, Kim CJ. Creating transporting, cutting, and merging liquid droplets by electrowetting-based actuation for digital microfluidic circuits. J Microelectromech Syst. 2003;12(1):70–80.
[8] Chakrabarty K, Xu T. Digital microfluidic biochips: design automation and optimization. Los Angeles: CRC Press; 2010.
[9] Rose D. Microdispensing technologies in drug discovery. Drug Discov Today. 1999;4(9):411–9.
[10] Ren H, Fair RB, Pollack MG. Automated on-chip droplet dispensing with volume control by electro-wetting actuation and capacitance metering. Sens Actuators B Chem. 2004;98(2–3):319–27.
[11] Fair RB. Digital microfluidics: is a true lab-on-a-chip possible. Microfluid Nanofluid. 2007;3(3):245–81.
[12] Li Y, Baker RJ, Raad D. A highly efficient and reliable electrowetting on dielectric device for point-of-care diagnostics. Proceeding of 2015 IEEE Dallas Circuits and Systems Conference (DCAS), Dallas, TX, USA. Piscataway: IEEE; 2015 Oct 12–13. p. 1–4.
[13] Kim H, Bartsch MS, Renzi RF, He J, Vreugde JLV, Claudnic MR, et al. Automated digital microfluidic sample preparation for next-generation DNA sequencing. J Lab Autom. 2011;16(6):405–14.

[14] Ding H, Sadeghi S, Shah GJ, Chen S, Keng PY, Kim CJ, et al. Accurate dispensing of volatile reagents on demand for chemical reactions in EWOD chips. Lab Chip. 2012;12(18):3331–40.
[15] Ren H, Fair RB. Micro/Nano liter droplet formation and dispensing by capacitance metering and electrowetting actuation. Proceedings of the 2nd IEEE Conference on Nanotechnology, Washington, DC, USA. Piscataway: IEEE; 2002 Aug 28. p. 369–72.
[16] Gong J, Kim CJ. Real-time feedback control of droplet generation for EWOD digital microfluidics. Proceedings of the 10th International Conference on Miniaturized Systems for Chemistry and Life Sciences (μTAS), Tokyo, Japan. Pittsburgh: Chemical and Biological Microsystems Society; 2006 Nov 5–9. p. 1046–8.
[17] Gong J, Kim CJ. Characterization and design of digitizing process for uniform and controlable droplet volume in EWOD digital microfluidics. Proceedings of Solid-State Sensors, Actuators, and Microsystems Workshop. Hilton Head Island, SC, USA; 2006 Jun 4–8. p. 159–62.
[18] Yaddessalage JB. Study of the capabilities of electrowetting on dielectric digital microfluidics (EWOD DMF) towards the high efficient thin-film evaporative cooling platform. Arlington: The University of Texas at Arlington; 2013.
[19] Nikapitiya NYJB, Nahar MM, Moon H. Accurate, consistent, and fast droplet splitting and dispensing in electrowetting on dielectric digital microfluidics. Micro and Nano Syst Lett. 2017;5(1):24.
[20] Dong C, Jia Y, Gao J, Chen T, Mak P, Vai M, et al. A 3D microblade structure for precise and parallel droplet splitting on digital microfluidic chips. Lab Chip. 2017;17(5):896–904.
[21] Wang W, Jones TB, Harding DR. On-chip double emulsion droplet assembly using electrowetting-on-dielectric and dielctrophoresis. Fusion Sci Technol. 2001;59(1):240–9.
[22] Walker SW, Shapiro B. Modeling the fluid dynamics of electrowetting on dielectric (EWOD). J Microelectromech S. 2006;15(4):986–1000.
[23] Jin C, Xiong X, Patra P, Zhu R, Hu J. Design and simulation of high-throughput microfluidic droplet dispenser for lab-on-a-chip applications. Proceedings of the 2014 COMSOL Conference, Boston, US. Stockholm: COMSOL; 2014 Oct 7–9. p. 1–7.
[24] Wang H, Chen L. Electrowetting-on-dielectric based economical digital microfluidic chip on flexible substrate by inkjet printing. Micromachines. 2020;11(12):1113.